Scanning Tunneling Microscopy Contrast Mechanisms for TiO_2

T. Woolcot,[1,2] G. Teobaldi,[3,*] C. L. Pang,[1,2] N. S. Beglitis,[1,4] A. J. Fisher,[1,4] W. A. Hofer,[3] and G. Thornton[1,2,†]

[1]*London Centre for Nanotechnology, 17–19 Gordon Street, London WC1H 0AH, United Kingdom*
[2]*Department of Chemistry, University College London, 20 Gordon Street, London WC1H OAJ, United Kingdom*
[3]*Stephenson Institute for Renewable Energy and Surface Science Research Centre, Department of Chemistry, University of Liverpool, Liverpool L69 3BX, United Kingdom*
[4]*Department of Physics and Astronomy, University College London, Gower Street, London WC1E 6BT, United Kingdom*

(Received 13 July 2012; revised manuscript received 26 August 2012; published 12 October 2012)

Controlled dual mode scanning tunneling microscopy (STM) experiments and first-principles simulations show that the tunneling conditions can significantly alter the positive-bias topographic contrast of geometrically corrugated titania surfaces such as rutile $TiO_2(011)$-(2×1). Depending on the tip-surface distance, two different contrasts can be reversibly imaged. STM simulations which either include or neglect the tip-electronic structure, carried out at three density functional theory levels of increasing accuracy, allow assignment of both contrasts on the basis of the $TiO_2(011)$-(2×1) structure proposed by Torrelles *et al.* [Phys. Rev. Lett. **101**, 185501 (2008)]. Finally, the mechanisms of contrast formation are elucidated in terms of the subtle balance between the surface geometry and the different vacuum decay lengths of the topmost Ti($3d$) and O($2p$) states probed by the STM-tip apex.

DOI: 10.1103/PhysRevLett.109.156105 PACS numbers: 68.35.B−, 68.37.Ef, 68.47.Gh

Scanning tunneling microscopy (STM) is an extremely powerful tool for examining the geometric and electronic structure of surfaces, both with and without the presence of adsorbates. An understanding of the atomic and electronic structure of nanostructured surfaces and interfaces is crucial for controlling their functionality in novel applications. Unfortunately, for compound surfaces such as metal oxides, the assignment of STM features is far from straightforward, and our knowledge of the contrast formation mechanism for this class of substrates is still disappointingly poor. Despite the role of TiO_2 as a model metal oxide [1,2], and its extensive use in many energy relevant applications [1,3], only the STM appearance of the rutile (110) face is currently well understood [4–9], with good agreement between the experimental and simulated STM images.

The (011) face of rutile TiO_2 has attracted much attention recently. It forms the second most abundant face of the equilibrium rutile crystal [10], and has been reported to exhibit an enhanced photocatalytic response [11]. After routine preparation in ultrahigh vacuum (UHV) conditions, the surface forms a 2×1 reconstruction [12–16], the structure of which has only recently been solved with surface x-ray diffraction (SXRD) and density functional theory (DFT) calculations [17,18]. Although the surface crystallography appears to be now understood, there is a significant discrepancy between the STM experiment and simulation of this surface. Resolving this discrepancy is the major goal of this Letter.

Most of the available positive-bias (empty states) STM images of the $TiO_2(011)$-(2×1) surface show the appearance of zigzag rows of round features [12–15]. A second imaging mode, characterized by the appearance of rows of staggered beanlike features has been recently reported by Gong *et al.* [18]. After inspecting numerous images taken from two different STM instruments, it was concluded that those taken at low bias voltages are more often of the beanlike contrast, whereas large bias positive imaging of the surface leads predominantly to the zigzag rows being observed [18]. Despite successful reproduction of the beanlike contrast, simulation of the local density of states above the SXRD-derived model could not reproduce the most generally observed zigzag contrast [12–15,18], which leaves the latter currently unassigned. The rapidly growing number of STM-based studies of molecular adsorption on the substrate imaged in the zigzag mode [19–21] makes the lack of atomic assignment for this contrast especially unfortunate, and may raise questions about the accuracy of the SXRD- and DFT-derived surface structure [17,18] and, consequently, of the adsorbate induced reconstructions recently proposed for the substrate [21,22].

Here, by interplay between experiment and simulations with inclusion of the STM tip, we show the SXRD-based model to be fully compatible with the two reported STM contrasts, and provide atomic assignment for the zigzag imaging mode of $TiO_2(011)$. Experimental STM images were simultaneously recorded at high and low bias. The high bias images gave the zigzag appearance, whereas the low bias images were beanlike. STM simulations which either include or neglect the tip electronic structure, carried out within three different DFT approaches of increasing accuracy and computational cost, allow rationalization of the experimental findings on the basis of the subtle balance between surface electronic and geometrical factors, and the non-negligible role of the STM-tip electronic structure for the STM appearance of $TiO_2(011)$. These results highlight

elements, so far overlooked, which should be useful for future STM investigations of TiO_2 and other metal-oxide based surfaces.

STM images of $TiO_2(011)$ (PiKem) were recorded using an Omicron LT UHV STM operated at 78 K, with tips made from electrochemically etched tungsten wire. Prior to imaging, the sample was prepared by cycles of 1 kV Ar^+ bombardment at 45° incidence and annealing to 1100 K. Surface cleanliness and long range order were confirmed with x-ray photoelectron spectroscopy (XPS) and low energy electron spectroscopy (LEED).

Figure 1 shows empty state constant-current STM images of the surface obtained during dual mode scanning. Dual mode scanning simply allows the tunneling parameters to be set separately for the forward and backward components of the raster scan of the surface, with a scan line delay of ~1 ms. The two images are therefore effectively obtained simultaneously, with an identical tip-surface system throughout. Over the course of the experiment, the two contrasts were found to be reversibly reproducible using the optimal parameters shown.

Measurement of the interfeature distances of the zigzag mode clearly indicates that such contrast cannot be due to geometric factors alone. If an isosceles triangle is positioned on the STM array of bright features as in Fig. 1, then the average vertex angle is 93.6° ± 0.9° and the diagonal interfeature separation is 3.7 ± 0.1 Å. This geometry differs from any of the in-plane projections between equivalent topmost sites of the experimental model [17]: Ti(1/1*) = 2.97 Å, O(1/1*) = 2.90 Å, and O(2/2*) = 5.53 Å (Fig. 2). This demonstrates that the STM zigzag contrast is largely electronically derived.

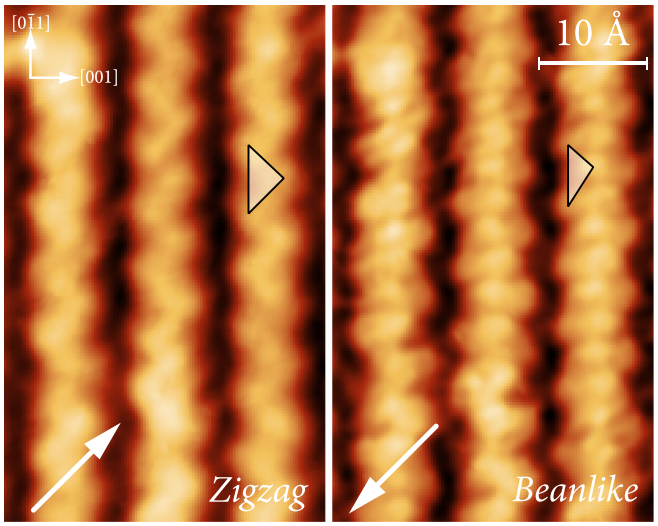

FIG. 1 (color online). Forward and backward scans of the same region recorded simultaneously during dual mode STM. The zigzag and beanlike images were obtained at large (1.7 V, 0.5 nA) and small (1.1 V, 1.5 nA) tip-sample distances, respectively. Images are rotated with arrows indicating the tip scan direction. Data were filtered using a box pass in the two-dimensional fast Fourier transform to remove high frequency noise only.

For the staggered bean mode, the equivalent measurement is of a scalene triangle of vertex angle 109.0° ± 2.7° with interfeature distances 3.1 ± 0.1 Å and 3.6 ± 0.1 Å. Within error, these values closely match the experimental in-plane projections between the O(1) and O(2) atoms: 2.98 and 3.72 Å (Fig. 2). This suggests that geometric factors have a predominant role in the imaging of the bean-shaped contrast. However, consistent with its nonuniformity (Fig. 1 and Ref. [18]), and the close tip-sample separation (estimated at 2–3 Å from Ref. [18] and Fig. 3), we found the bean-shaped imaging mode to be heavily dependent on the details of the tip-apex structure, and expect it to be of limited use for the study of molecular adsorption on $TiO_2(011)$-(2 × 1).

To gain insight into the formation of the two W-tip STM contrasts, the STM imaging of the surface was simulated on the basis of both the Tersoff-Hamann (TH) [23] and Bardeen [24] approximations, as implemented in the BSKAN code [25–27]. The contribution of the tip-electronic structure to the image formation is included in the Bardeen method but not in the TH method (see the Supplemental

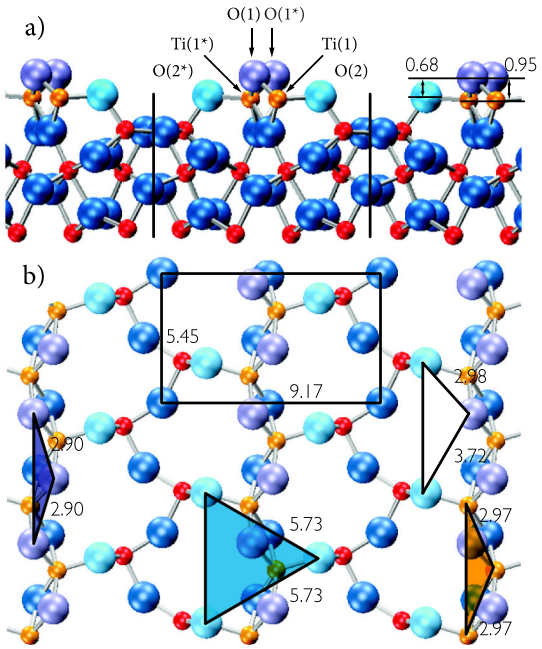

FIG. 2 (color online). Side (a) and top (b) view of the $TiO_2(011)$-(2 × 1) surface and adopted labeling. The O and Ti atoms are displayed as large and small balls, respectively. For clarity, only the two (three) topmost Ti and (O) layers have been shown in (b). The (2 × 1) unit cell is highlighted in (b), as are the in-plane geometries of the topmost Ti(1/1*), O(1/1*), and O(2/2*) atoms (colored triangles) for comparison with STM. The unfilled triangle shows the in-plane distances between the O(1) and O(2) atoms, which are in close agreement with the experimental geometry of the beanlike mode. The azimuths are as in Fig. 1 and distances shown are in angstrom.

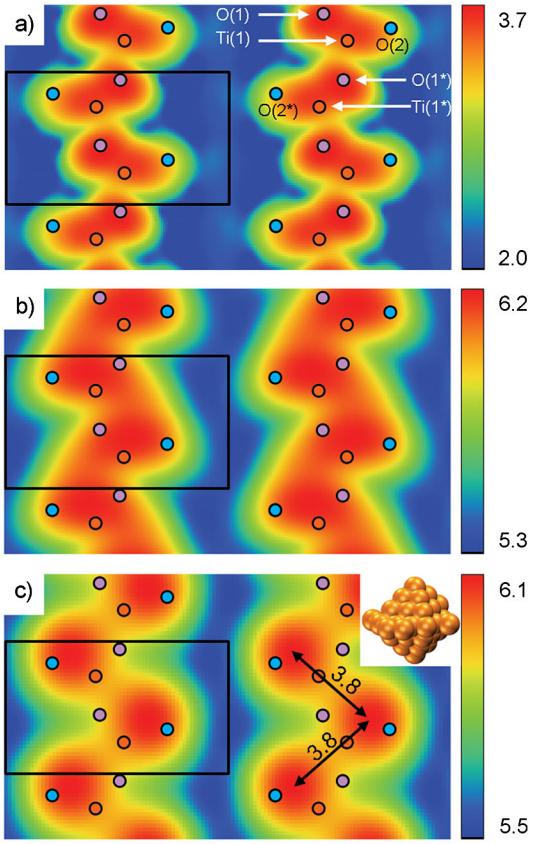

FIG. 3 (color online). The simulated HSE06 TH STM images at different heights (Å) above the surface [(a) 1.1 V, 5×10^{-5} e Å^{-3}, (b) 1.1 V, 10^{-7} e Å^{-3}]. (c) The simulated W-tip HSE06 Bardeen image at 1.1 V and 0.05 nA. The bipyramid W-tip model is displayed in the inset. The top- and bottommost atoms form the two tip apexes. The atomic sites are marked by circles and labeled as in Fig. 2. The arrows in (c) mark the in-plane distance (Å) between the modeled brightest features.

Material [28]). The advantage of this procedure, neglected in Ref. [18], is that it is possible to assess directly the role of the tip-electronic structure in the STM contrast formation by comparison between the Bardeen and TH results. For consistency between the different DFT approaches used, in all cases the bias was referenced to the onset of the conduction band (CB).

The surface was simulated by the same eight-layer slab previously adopted in Ref. [17], and the W STM tip by the same atomically ended, periodically repeated W(110) bipyramid model previously used and characterized in Refs. [6,29,30]. To investigate the effect of the electronic structure treatment on the description of Ti(3d) states and hence on the simulated STM contrast, the surface electronic structure was optimized at three different DFT levels: using the generalized gradient approximation (PBE) [31] (on the PBE-optimized geometry), screened hybrid DFT (HSE06) [32] (also on the PBE-optimized geometry), and the LSDA + U method [33] (on the LSDA + U optimized geometry), as implemented in the VASP program [34,35]. In the LSDA + U simulations we took $U =$ 5.5 eV, proposed on the basis of coupled-cluster simulations of fivefold coordinated Ti atoms in rutile TiO_2 [36]. We note that, to the best of our knowledge, the LSDA + U and hybrid-DFT methods have not been previously applied to the TiO_2(011)-(2 × 1) surface. Further details on both the DFT and STM simulations can be found in the Supplemental Material [28].

Figures 3(a) and 3(b) report the simulated HSE06 TH imaging at different heights above the surface. Consistent with previous PBE results [18], and regardless of the DFT flavor, we find that the bright bean-shaped features are located close to the topmost O(1/1*) atoms for small tip-surface distances [Fig. 3(a)], and extend towards the in-plane projection of O(2/2*). However, as the tip-surface distance is increased [Fig. 3(b)], the simulated contrast progressively changes into a sharpened zigzag pattern, much closer to the experimental contrast imaged for larger tip-surface distances (Fig. 1 and Ref. [18]). In this case, the brightest features are centered close to the topmost Ti(1) [Ti(1*)] atoms, roughly between the in-plane projection of the O(1) [O(1*)] and O(2) [O(2*)] atoms.

The simulations allow us to rationalize the experimental change of contrast on the basis of three different competing factors: namely, (i) the conduction band composition, (ii) the surface geometry, and (iii) the different vacuum decay lengths of Ti(3d) and O(2p) electronic states. As shown in the Supplemental Material [28], the TiO_2(011)-(2 × 1) CB is dominated by Ti(3d) states, with smaller, yet nonzero, contributions from O(2p) states. Thus, positive-bias bright features should correspond to the accumulation of Ti(3d) states, as for the TiO_2(110) surface [4–7]. However, the topmost Ti(1/1*) atoms lie 0.95 Å below the topmost O(1/1*) atoms (Fig. 2). Depending on the different contributions of Ti(3d) and O(2p) states to the CB [factor (i)], and their different vacuum decay (see below), this element favors imaging of O(2p) states for small tip-surface distances. Finally, due to a longer vacuum decay length, Ti(3d) electronic states outside the surface extend into the vacuum more than O(2p) states [4–7]. Thus, provided the tip-surface distance is sufficiently large to allow extinction of the O(2p) states (see the Supplemental Material [28]), and in spite of the surface geometry [factor (ii)], slow-decaying Ti(3d) states can overcome fast-decaying O(2p) states and be imaged as bright features in positive-bias STM images. Hence, we find the positive-bias STM contrast of TiO_2(011) to be governed by exactly the same factors as for TiO_2(110), where Ti(3d) states from fivefold coordinated Ti atoms are imaged as bright features [4–7], even though they lie 1.13 Å lower on the surface.

For the interested reader, we also note that, in the TH-PBE simulations, the contrast is lost as the tip-surface distance is increased and the change of contrast is not reproduced. This behavior is at odds with that found using

HSE06 (Fig. 3) and LSDA + U (see the Supplemental Material [28]), and originates from the larger contribution of O($2p$) states to the CB (see the Supplemental Material [28]), when using the PBE approximation, which prevents the emergence of the zigzag contrast at large tip-surface distances. These results suggest that the hybrid-DFT and LSDA + U methods improve the description of the vacuum decay of the TiO_2(011)-(2 × 1) electronic states with respect to the PBE approximation.

An interesting detail of the experimental images in Fig. 1 is the rounded appearance of the bright features for the large-distance zigzag contrast. Given the distorted fivefold (twofold) connectivity of the top-most Ti (O) atoms, this suggests that tip-convolution smoothing effects could affect the STM acquisition. This, together with the noticeably less rounded appearance of the simulated TH features at large distances (Fig. 2), prompted us to consider explicitly the role of the tip electronic structure in the STM imaging of the surface [37].

Figure 3(c) shows the positive-bias STM appearance of TiO_2(011) in the Bardeen model together with the atomically sharp W-tip model that was used. Inclusion of the W tip in the simulations allows full recovery of the experimentally observed zigzag pattern (Fig. 1). Convolution effects due to the finite electronic sharpness of the STM tip (see the Supplemental Material [28] and Ref. [30] lead to rounding of the bright features and their partial shift towards the projection of the O($2/2^*$) atoms, farther from the topmost O($1/1^*$) atoms than in the TH case. The very good agreement obtained for the in-plane distance of the brightest feature (theory: 3.8 Å in Fig. 3; experiment: 3.7 ± 0.1 Å in Fig. 1) supports both the simulation protocol and our proposed assignment of the zigzag contrast. LSDA + U based Bardeen simulations (see the Supplemental Material [28]) recover qualitatively similar results. Importantly, different filtering of the Ti($3d$) and O($2p$) states by the tip electronic structure leads to the appearance of a zigzag pattern in close agreement with experiment also for the PBE case (see the Supplemental Material [28]). Thus, provided the tip electronic structure is accounted for, the large tip-surface distance zigzag contrast of TiO_2(011) can be qualitatively reproduced also on the basis of computationally less expensive PBE-based simulations.

Tip effects on the STM appearance of rutile TiO_2(110) as a function of the tip-surface distance have been previously investigated in Refs. [7–9]. There, it was found acceptable to consider fixed tip and surface geometries for tunneling current evaluation at tip-surface distances larger than 3 Å. These findings support the use of the Bardeen method in the present case, especially since the calculated Bardeen tip-surface distance for the considered tunneling conditions was always larger than 5 Å {see Fig. 3(c) and the Supplemental Material [28]}.

To summarize, an experimental and theoretical investigation of TiO_2(011) positive-bias STM imaging confirms the existence of two contrasts. The appearance of the staggered bean-shape pattern is assigned to imaging of the topmost O-atoms for close tip-surface distances. The rounded features of the more commonly imaged zigzag contrast are shown to originate from Ti($3d$) states of the topmost fivefold coordinated Ti atoms. Both contrasts are rationalized in terms of the competition between the longer vacuum decay length of Ti($3d$) states with respect to O($2p$) states on one hand, and the surface geometry on the other (the topmost O atoms being more exposed than Ti atoms). The tip electronic structure is shown to affect crucially the contrast at large tip-surface distances, especially if generalized gradient corrected functionals (such as the PBE approximation) are used. These results should be useful for the interpretation of the increasingly large number of STM investigations of molecular adsorption on TiO_2(011) and other corrugated titania faces.

This work was supported by EPSRC-UK (EP/I004483/1, EP/C541898/1) and by a European Research Council Advanced Grant (to G. Thornton). The authors are grateful to Robert Lindsay and Xavier Torrelles for making the experimental model of the surface available.

*g.teobaldi@liv.ac.uk
†g.thornton@ucl.ac.uk

[1] U. Diebold, Surf. Sci. Rep. **48**, 53 (2003).
[2] C. L. Pang, R. Lindsay, and G. Thornton, Chem. Soc. Rev. **37**, 2328 (2008).
[3] M. A. Henderson, Surf. Sci. Rep. **66**, 185 (2011).
[4] U. Diebold, J. F. Anderson, K.-O. Ng, and D. Vanderbilt, Phys. Rev. Lett. **77**, 1322 (1996).
[5] U. Diebold, J. Lehman, T. Mahmoud, M. Kuhn, G. Leonardelli, W. Hebenstreit, M. Schmid, and P. Varga, Surf. Sci. **411**, 137 (1998).
[6] G. Teobaldi, W. A. Hofer, O. Bikondoa, C. L. Pang, G. Cabailh, and G. Thornton, Chem. Phys. Lett. **437**, 73 (2007).
[7] C. Sánchez-Sánchez, C. González, P. Jelinek, J. Méndez, P. L. de Andres, J. A. Martín-Gago, and M. F. López, Nanotechnology **21**, 405702 (2010).
[8] G. H. Enevoldsen, H. P. Pinto, A. S. Foster, M. C. R. Jensen, A. Kühnle, M. Reichling, W. A. Hofer, J. V. Lauritsen, and F. Besenbacher, Phys. Rev. B **78**, 045416 (2008).
[9] H. P. Pinto, G. H. Enevoldsen, F. Besenbacher, J. V. Lauritsen, and A. S. Foster, Nanotechnology **20**, 264020 (2009).
[10] M. Ramamoorthy, D. Vanderbilt, and R. D. King-Smith, Phys. Rev. B **49**, 16721 (1994).
[11] T. Ohno, K. Sarukawa, and M. Matsumura, New J. Chem. **26**, 1167 (2002).
[12] T. J. Beck, A. Klust, M. Batzill, U. Diebold, C. Di Valentin, and A. Selloni, Phys. Rev. Lett. **93**, 036104 (2004).
[13] T. Kubo, H. Orita, and H. Nozoye, J. Am. Chem. Soc. **129**, 10474 (2007).

[14] O. Dulub, C. Di Valentin, A. Selloni, and U. Diebold, Surf. Sci. **600**, 4407 (2006)
[15] O. Dulub, M. Batzill, S. Solovev, E. Loginova, A. Alchagirov, T. E. Madey, and U. Diebold, Science **317**, 1052 (2007).
[16] S. E. Chamberlin, C. J. Hirschmugl, H. C. Poon, and D. K. Saldin, Surf. Sci. **603**, 3367 (2009).
[17] X. Torrelles, G. Cabailh, R. Lindsay, O. Bikondoa, J. Roy, J. Zegenhagen, G. Teobaldi, W. A. Hofer, and G. Thornton, Phys. Rev. Lett. **101**, 185501 (2008).
[18] X. Gong, N. Khorshidi, A. Stierle, V. Vonk, C. Ellinger, H. Dosch, H. Cheng, A. Selloni, Y. He, O. Dulub, and U. Diebold, Surf. Sci. **603**, 138 (2009).
[19] A. Tekiel, S. Godlewski, J. Budzioch, and M. Szymonski, Nanotechnology **19**, 495304 (2008).
[20] J. Tao, T. Luttrell, J. Bylsma, and M. Batzill, J. Phys. Chem. C **115**, 3434 (2011).
[21] Q. Cuan, J. Tao, X.-Q. Gong, and M. Batzill, Phys. Rev. Lett. **108**, 106105 (2012).
[22] U. Aschauer and A. Selloni, Phys. Rev. Lett. **106**, 166102 (2011).
[23] J. Tersoff and D. R. Hamann, Phys. Rev. B **31**, 805 (1985).
[24] J. Bardeen, Phys. Rev. Lett. **6**, 57 (1961).
[25] W. Hofer and J. Redinger, Surf. Sci. **447**, 51 (2000).
[26] W. A. Hofer, Prog. Surf. Sci. **71**, 147 (2003).
[27] K. Palotás and W. A. Hofer, J. Phys. Condens. Matter **17**, 2705 (2005).
[28] See Supplemental Material at http://link.aps.org/supplemental/10.1103/PhysRevLett.109.156105 for supplementary methods and results.
[29] G. Teobaldi, M. Peñalba, A. Arnau, N. Lorente, and W. A. Hofer, Phys. Rev. B **76**, 235407 (2007).
[30] G. Teobaldi, E. Inami, J. Kanasaki, K. Tanimura, and A. L. Shluger, Phys. Rev. B **85**, 085433 (2012).
[31] J. P. Perdew, K. Burke, and M. Ernzerhof, Phys. Rev. Lett. **77**, 3865 (1996).
[32] J. Heyd, G. E. Scuseria, and M. Ernzerhof, J. Chem. Phys. **118**, 8207 (2003); **124**, 219906 (2006).
[33] S. L. Dudarev, G. A. Botton, S. Y. Savrasov, C. J. Humphreys, and A. P. Sutton, Phys. Rev. B **57**, 1505 (1998).
[34] G. Kresse and J. Hafner, Phys. Rev. B **47**, 558 (1993).
[35] G. Kresse and J. Furthmüller, Phys. Rev. B **54**, 11169 (1996).
[36] C. J. Calzado, N. C. Hernández, and Javier Fdez. Sanz, Phys. Rev. B **77**, 045118 (2008).
[37] The limitations of the Bardeen method (see the Supplemental Material [28]) prevent meaningful simulation of the close-distance bean-shaped contrast. Given the arguably strong dependence of this contrast on the detailed structure of the STM tip, its limited use in studying molecular adsorption on TiO_2(011) [19–21], and the computational cost of STM simulations in the strong tip-surface interaction regime [7], we leave the study of tip effects on the close-distance bean-shaped STM contrast to future investigations.